

PACS numbers: 61.05.cp, 68.37.Hk, 78.30.-j, 81.15.Cd, 82.80.Pv, 88.40.fh, 88.40.jn

Non-Vacuum Design of $\text{CuGa}_x\text{In}_{1-x}\text{Se}_2$ Films for Solar Energy Applications

S. S. Kovachov, K. M. Tikhovod, M. V. Kalenyk*, I. T. Bohdanov, and
Ya. O. Sychikova

Berdyansk State Pedagogical University,
4, Schmidt Str.,
71100 Berdyansk, Ukraine

**Sumy State Pedagogical University named after A. S. Makarenko,*
87, Romenska Str.,
40002, Sumy, Ukraine

The study reports on a non-vacuum synthesis method for $\text{CuGa}_x\text{In}_{1-x}\text{Se}_2$ films for solar energy applications. The films are formed by pulverising chlorides of indium, gallium, and cuprum with selenious acid. To optimise the blend composition of films, it is proposed to age the obtained structure in a sodium chloride solution and to carry out additional selenization of the surface in a diffusion furnace. The resulting layers are investigated using SEM, EDX, XRD, and Raman methods. As determined, the film is a polycrystalline structure of chalcopyrite $\text{CuGa}_{0.6}\text{In}_{0.4}\text{Se}_2$ with agglomerates of porous crystallites. Secondary phases are not detected. The proposed method does not require a vacuum, and it is simple and inexpensive that opens the prospect of using it on an industrial scale for the synthesis of $\text{Cu}_x\text{GaIn}_{1-x}\text{Se}_2$ metal films.

Key words: pulverising, chalcopyrite, thin films, solar batteries, selenides, copper.

У роботі повідомляється про безвакуумний метод синтези плівок $\text{CuGa}_x\text{In}_{1-x}\text{Se}_2$ для застосувань у сонячній енергетиці. Плівки було сформовано методом пульверизації хлоридів Індію, Галію та Купруму з селеністою кислотою. Для оптимізації компонентного складу плівок запро-

Corresponding author: Yana Oleksandrivna Sychikova
E-mail: yanasuchikova@gmail.com

Citation: S. S. Kovachov, K. M. Tikhovod, M. V. Kalenyk, I. T. Bohdanov, and
Ya. O. Sychikova, Non-Vacuum Design of $\text{CuGa}_x\text{In}_{1-x}\text{Se}_2$ Films for Solar Energy Appli-
cations, *Metallofiz. Noveishie Tekhnol.*, **45**, No. 5: 593–602 (2023).
DOI: [10.15407/mfint.45.05.0593](https://doi.org/10.15407/mfint.45.05.0593)

поновано витримувати одержану структуру у розчині хлориду Натрію та проводити додаткову селенізацію поверхні у дифузійній печі. Одержані шари було досліджено за допомогою SEM, EDX, XRD та Raman методів. Встановлено, що плівка представляє собою полікристалічну структуру халькопіриту $\text{CuGa}_{0.6}\text{In}_{0.4}\text{Se}_2$ з агломератами поруватих кристалітів. Другорядних фаз не було зафіксовано. Запропонований метод не потребує вакууму, є простим і недорогим, що відкриває перспективи використання його у промислових масштабах для синтезу плівок $\text{CuGa}_x\text{In}_{1-x}\text{Se}_2$.

Ключові слова: пульверизація, халькопірит, тонкі плівки, сонячні батареї, селеніди, мідь.

(Received February 15, 2023; in final version, February 28, 2023)

1. INTRODUCTION

Semiconductors based on gallium and indium have become popular due to their wide application prospects in laser technology [1], sensorics [2], solar energy [3], *etc.* Today, many studies focus on studying the phase states of these semiconductors [4, 5], their optical properties [6, 7], and their methods of integration with other semiconductors [8, 9]. The interest in these semiconductors is also due to the simplicity of nanostructuring of their surface [10–12]. Thus, the synthesis of porous layers [13], nanoneedles [14], nanowhiskers [15], quantum dots [16], microcrystallites [17], *etc.* has been reported many times.

Recently, ternary metal compounds, particularly those containing copper, have been actively studied, including CuZnSe_2 [18], CuInSe_2 [19], and CuIn(Ga)Se_2 [20]. Copper indium (gallium) (di)selenide (CIS), CuIn(Ga)Se_2 , is an important semiconductor for the production of thin-film solar cells [21–23]. It is characterised by a high optical absorption index and long-term stability [24, 25], which allows it to be used as a reliable absorbing layer.

$\text{CuIn}_x\text{Ga}_{x-1}\text{Se}_2$ was obtained by magnetron sputtering [26], evaporation [27], deposition [28, 29], *etc.* However, vacuum methods have a number of disadvantages, including a high processing temperature, high-energy requirements, and the need to use high-tech equipment and ultrapure materials. In turn, this leads to a high cost of the resulting material and decreases the chances of its introduction into the solar energy sector.

In this regard, the attention of researchers has been focused on electrochemical deposition methods [30], solvothermal methods [31], and SILAR [32]. In addition, combined methods are becoming popular, such as electrochemical etching with simultaneous deposition and a sol-gel method with thermal annealing. In this case, such a problem arises as the control of the content of Cu and In metals [33, 34]. This can lead to excessive conductivity of the obtained layers, which nega-

tively affects the efficiency of photovoltaic energy converters based on $\text{Cu}(\text{In}, \text{Ga})\text{Se}_2$ structures [35, 36]. To remove this effect, researchers have suggested additional doping of synthesised films [37, 38]. In particular, Na doping has become popular, which improves the morphological characteristics of films and their optical properties [39].

In this study, we describe a simple method for the synthesis of polycrystalline $\text{CuIn}_x\text{Ga}_{x-1}\text{Se}_2$ and investigate its structural, component, and morphological characteristics.

2. EXPERIMENTAL/THEORETICAL DETAILS

2.1. Samples for the Experiment

As precursors, the chlorides of copper, indium, and gallium were used as sources of copper, indium, and gallium, respectively. Oleic acid was also used as an organic solvent, and selenious acid was used as a source of selenium (see Table 1). In the experimental process, CuCl_2 , InCl_3 , GaCl_3 , and H_2SeO_3 (a chemical mixture) were mixed in a ratio of 1:0.6:0.4:2 in oleic acid using a magnetic stirrer for 20 min.

2.2. Methods and Conditions of the Experiment

$\text{CuGa}_x\text{In}_{1-x}\text{Se}_2$ films were formed by the method of liquid phase pulverization (a spray-pyrolysis). The experimental device was equipped with a heating system that allows heating both the liquid phase and the substrate. The substrate temperature was constant throughout the duration of the experiment. The system was also equipped with an exhaust fan to remove gaseous reaction by products. Compressed air was used as the carrier gas. Spray speed and pressure were kept constant throughout the duration of the experiment. Other conditions of the experiment are given in Table 2.

After deposition, the samples were immersed in NaCl solution for 20 min. Subsequently, additional selenization was carried out in a Jet-First diffusion furnace at a temperature of 530°C for 30 minutes to ensure grain growth and compaction of films of high crystallinity. After

TABLE 1. Precursors used in the experiment.

| No. | Precursor | Characteristic |
|-----|--|----------------|
| 1 | CuCl_2 | Anhydrous, 98% |
| 2 | InCl_3 | Anhydrous, 98% |
| 3 | GaCl_3 | Anhydrous, 99% |
| 4 | H_2SeO_3 | Anhydrous, 98% |
| 5 | $\text{C}_{18}\text{H}_{34}\text{O}_2$ | Anhydrous, 98% |

TABLE 2. Experimental conditions for deposition of $\text{CuGa}_x\text{In}_{1-x}\text{Se}_2$ films.

| Parameter | Value |
|---|----------|
| Substrate temperature | 320°C |
| The distance between a substrate and a nozzle | 20 cm |
| Spraying speed | 3 ml/min |
| Spraying time | 10 min |
| Carrier gas pressure | 3.5 MPa |

that, they were cooled to room temperature.

2.3. Characterization

The surface morphology was studied with a SEO-SEM Inspect S50-B scanning electron microscope. Energy-dispersive x-ray microanalysis (EDX) was used to analyse the chemical composition of the deposited films using the AZtecOne detector. To improve the reliability of EDX, this analysis was performed at an accelerating voltage of 15 kV in large areas of 200 μm^2 .

For x-ray structural analysis, a Dron-3M diffractometer with unfiltered CuK_α radiation was used in the range of angles 2θ 10°–80° in increments of 0.1°. Raman spectroscopy measurements were performed at room temperature in the RENISHAW in Via Reflex system with an excitation wavelength of 532 nm at an intensity of 5%.

3. RESULTS AND DISCUSSION

3.1. SEM and EDX Analysis

In Figure 1, the SEM image of the formed film is shown. It can be seen that the surface relief is the agglomeration of disordered grains, which may indicate the polycrystalline nature of the formed structure. There is significant variation in the sizes of grains. The length of the crystallites varies in the range from 2 to 10 μm , and the width varies from 0.5 to 2 μm . The formed layer is loose. Crystallites have a significant number of pores on the surface. The transverse diameter is in the range of 80–140 nm. This, in turn, can lead to the appearance of quantum-dimensional effects.

The results of EDX analysis of the sample surface are shown in the Table 3. The values of $\text{Cu}/(\text{In} + \text{Ga})$ and $\text{Ga}/(\text{In} + \text{Ga})$ ratios were also calculated, which are 0.4 and 0.6, respectively. It can be seen that the additional selenization leads to a predominance of selenium on the sample surface. When it is considered that indium and gallium were sputtered

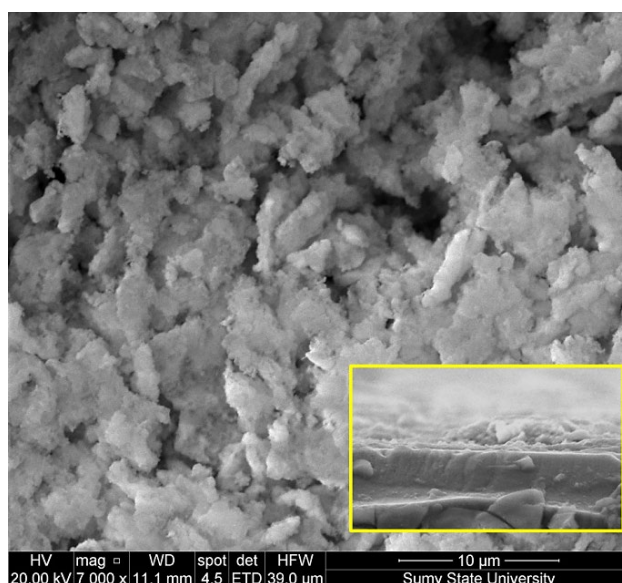


Fig. 1. XRD-spectrum of $\text{CuGa}_x\text{In}_{1-x}\text{Se}_2$.

TABLE 3. EDX analysis results for the $\text{CuGa}_x\text{In}_{1-x}\text{Se}_2$ film.

| Spectrum | Cu (at%) | In (at%) | Ga (at%) | Se (at%) | Cu/(In + Ga) | Ga (In + Ga) |
|----------|----------|----------|----------|----------|--------------|--------------|
| 1 | 16.82 | 14.18 | 21.26 | 47.74 | 0.47 | 0.6 |

in equal proportions, it can be assumed that selenization occurred due to the loss of In. Finally, it should be noted that Cu is also present in small concentrations.

3.2. XRD Analysis

The x-ray pattern of the synthesized $\text{CuGa}_x\text{In}_{1-x}\text{Se}_2$ film is shown in Fig. 2. The principal XRD peaks at 2θ 27.2° , 45.1° , 53.5° , and 65.7° belong to the (112), (211), (220), and (312) orientations of the structure of polycrystalline tetragonal chalcopyrite $\text{CuGa}_x\text{In}_{1-x}\text{Se}_2$. This indicates that the structure consisting of a polycrystalline $\text{CuGa}_x\text{In}_{1-x}\text{Se}_2$ film was successfully synthesised without the inclusion of additional phases.

The XRD spectra correspond to the compound formula $\text{CuGa}_{0.6}\text{In}_{0.4}\text{Se}_2$ (reference code: 00-035-1101). In Table 4, the principal XRD peaks and their correspondence to angles 2θ are shown.

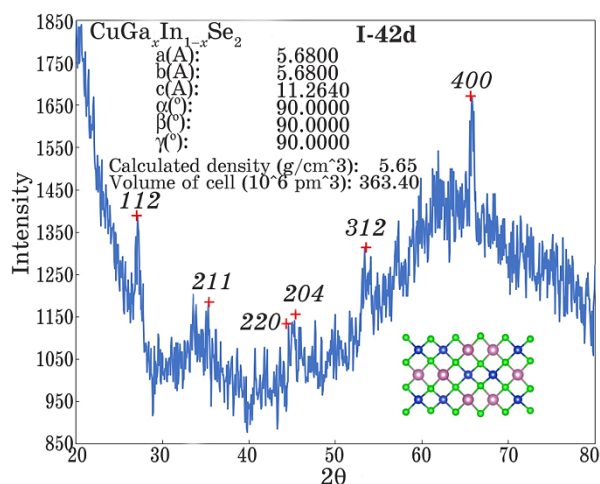


Fig. 2. XRD-spectrum of $\text{CuGa}_x\text{In}_{1-x}\text{Se}_2$.

TABLE 4. Crystal structure of $\text{CuGa}_{0.6}\text{In}_{0.4}\text{Se}_2$ determined by XRD spectrophotometry.

| No. | h | k | l | $d, \text{Å}$ | $2\theta, \text{deg}$ |
|-----|-----|-----|-----|---------------|-----------------------|
| 1 | 1 | 0 | 1 | 5.08 | 17.4 |
| 2 | 1 | 1 | 2 | 3.27 | 27.2 |
| 3 | 1 | 0 | 3 | 3.13 | 28.4 |
| 4 | 2 | 1 | 1 | 2.48 | 36.2 |
| 5 | 2 | 1 | 3 | 2.10 | 43.0 |
| 6 | 2 | 2 | 0 | 2.00 | 45.1 |
| 7 | 2 | 0 | 4 | 2.00 | 45.3 |
| 8 | 3 | 0 | 1 | 1.87 | 48.7 |
| 9 | 3 | 1 | 2 | 1.71 | 53.5 |
| 10 | 1 | 1 | 6 | 1.70 | 53.8 |
| 11 | 3 | 2 | 3 | 1.45 | 64.1 |
| 12 | 4 | 0 | 0 | 1.42 | 65.7 |
| 13 | 0 | 0 | 8 | 1.41 | 66.3 |
| 14 | 3 | 3 | 2 | 1.30 | 72.5 |
| 15 | 3 | 1 | 6 | 1.30 | 72.9 |

The x-ray pattern is characterised by a large amount of noise, which indicates a significant variation in the nanoparticle size and polycrystalline structure of the obtained film. This may also indicate the presence of an amorphous phase into which the crystal lattice is embedded.

3.3. Raman Analysis

The Raman spectrum of the obtained structure is shown in Fig. 3. We can see the presence of 2 high-intensity peaks, 3 medium-intensity peaks and a large number of low-intensity peaks. One of the most intense peaks at 175 cm^{-1} is associated with the $A1$ mode. This line is typical for AIBIIC2IV chalcopyrite compounds [40–42]. Other peaks, such as at 218 and 238 cm^{-1} , are significantly compatible with the $B2$ and E modes [43–46].

The largest peak at 190 cm^{-1} associated with the $A1$ mode of $\text{Cu}(\text{In}, \text{Ga})\text{Se}_2$ is due to the motion of the Se atom [40, 47]. The peaks at 136 and 150 cm^{-1} can be due to the effect of resonance enhancement of $\text{Cu}(\text{In}, \text{Ga})\text{Se}_2$ [48, 49]. The spectra of the leading secondary phases were not observed.

3.4. Discussion

Copper-containing solar batteries based on indium and gallium selenides have demonstrated their effectiveness and great potential in thin-film solar energy technologies. The creation of solar cells based on $\text{Cu}(\text{In}, \text{Ga})\text{Se}_2$ with an efficiency of up to 23% was reported [50]. In addition, such batteries have better radiation and thermal resistance and chemical stability [51]. Sophisticated and expensive methods for the synthesis of $\text{Cu}(\text{In}, \text{Ga})\text{Se}_2$ crystalline films are considered the main obstacle in the commercial use of chalcopyrite-based solar batteries. We have proposed a simple and inexpensive method of pulverisation

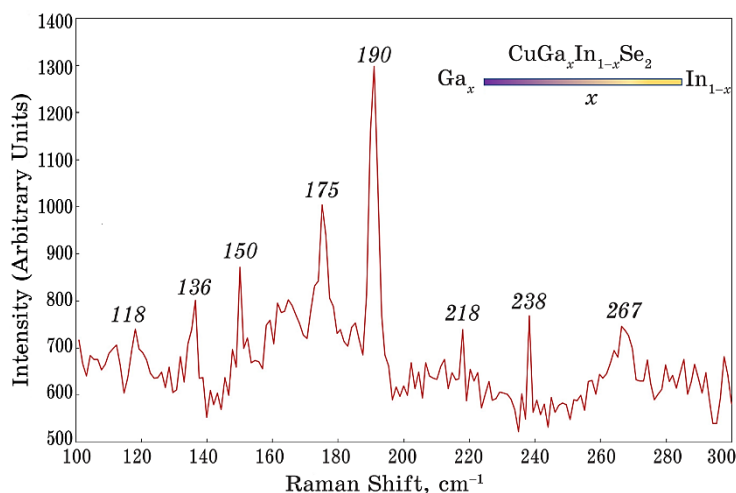


Fig. 3. Raman spectra of $\text{CuGa}_x\text{In}_{1-x}\text{Se}_2$.

that allows the deposition of thin nanostructured films on any substrate. The main advantage of the method is the absence of the necessity to use a vacuum and, therefore, expensive equipment.

The distinctive feature of this method is also the two-stage approach, which includes the deposition of metallic and non-metallic components with subsequent additional selenization to control the blend composition of the obtained compound. This allows the conductivity of the resulting film to be reduced due to selenium enrichment and removal of Cu_{2-x}Se phases. More research is necessary to determine the conditions for the formation of single-crystal $\text{CuGa}_x\text{In}_{1-x}\text{Se}_2$ films, as well as films with Cu and Se quantum dots.

4. CONCLUSION

We have demonstrated a simple method of obtaining $\text{CuGa}_x\text{In}_{1-x}\text{Se}_2$ crystal layers. The structure was formed by liquid phase pulverisation with the use of precursors of indium, gallium, cuprum chlorides, and selenious acid. After pulverization, the samples were subjected to sodium chloride, and additional selenization was performed in a diffusion furnace.

As a result, a dense layer of $\text{CuGa}_x\text{In}_{1-x}\text{Se}_2$ consisting of porous crystallites was obtained. EDX analysis showed that indium and gallium are in a 2:3 ratio. These data are significantly compliant with the results of XRD analysis. A Raman scattering study showed the absence of peaks of the Cu_2Se secondary phases. This indicates the effectiveness of the proposed synthesis technique and the prospects for its use on an industrial scale.

The study was supported by the Ministry of Education and Science of Ukraine (with projects No. 0122U000129, No. 0121U10942, No. 0123U100110). Yana Sychikova thankful for the support from COST Action CA20129 MultiChem.

We also thank the Armed Forces of Ukraine for the safety to carry out this work. This work was only possible thanks to the resilience and courage of the Ukrainian Army.

REFERENCES

1. F. Proise, F. Pardo, A. L. Joudrier, C. Njel, J. Alvarez, A. Delamarre, and J. L. Pelouard, *Simulation, and Photonic Engineering of Photovoltaic Devices III*, **8981**: 240 (2014).
2. S. Wang, Z. Zhou, B. Li, C. Wang, and Q. Liu, *Mater. Today Nano*, **16**: 100142 (2021).
3. Y. Suchikova, *East-Eur. J. Enterp. Technol.*, **6**, No. 5: 26 (2016).
4. A. Usseinov, Z. Koishybayeva, A. Platonenko, J. Purans, and A. I. Popov, *Ma-*

- terials*, **14**, Iss. **23**: 7384 (2021).
5. A. Usseinov, Z. Koishybayeva, A. Platonenko, Y. Suchikova, and A. I. Popov, *Latvian Journal of Physics and Technical Sciences*, **58**, Iss. **2**: 3 (2021).
 6. S. Yana, *Handbook of Nanoelectrochemistry: Electrochemical Synthesis Methods, Properties, and Characterization Techniques* (Springer: 2016), p. 1299.
 7. J. A. Suchikova, V. V. Kidalov, and G. A. Sukach, *ECS Transactions*, **25**, No. **24**: 59 (2009).
 8. T. Hidouri, H. Saidi, S. Nasr, I. Guizani, N. Ameer, F. Saidi, and H. Y. Zahran, *J. Electron. Mater.*, **51**: 3521 (2022).
 9. M. N. Hasan, Y. Zheng, J. Lai, E. Swinnich, O. G. Licata, M. A. Baboli, and J. H. Seo, *Adv. Mater. Interfaces*, **9**, Iss. **13**: 2101531 (2022).
 10. Y. Suchikova, S. Kovachov, A. Lazarenko, and I. Bohdanov, *Applied Surface Science Advances*, **12**: 100327 (2022).
 11. Y. Suchikova, S. Vambol, V. Vambol, N. Mozaffari, and N. Mozaffari, *J. Achievements in Materials and Manufacturing Engineering*, **92**, Iss. **1–2**: 19 (2019).
 12. A. Mangababu, R. S. P. Goud, C. Byram, J. Rathod, D. Banerjee, V. R. Soma, and S. N. Rao, *Appl. Surf. Sci.*, **589**: 152802 (2022).
 13. Y. A. Suchikova, V. V. Kidalov, and G. A. Sukach, *J. Nano-Electron. Phys.*, **2**, No. **4**: 75 (2010).
 14. S. O. Vambol, I. T. Bohdanov, V. V. Vambol, T. P. Nestorenko, and S. V. Onyschenko, *J. Nano-Electron. Phys.*, **9**, No. **6**: 06016 (2017).
 15. V. J. Gymez, M. Marnauza, K. A. Dick, and S. Lehmann, *Nanoscale Adv.*, **4**: 3330 (2022).
 16. M. Niu, K. Sui, X. Wu, D. Cao, and C. Liu, *Adv. Compos. Hybrid Mater.*, **5**: 450 (2022).
 17. Y. Suchikova, S. Kovachov, and I. Bohdanov, *Nanomater. Nanotechnol.*, No. **12** (2022).
 18. H. Ren, M. Wang, Z. Li, F. Laffir, G. Brennan, Y. Sun, and K. M. Ryan, *Chem. Mater.*, **31**, No. **24**: 10085 (2019).
 19. J. Du, R. Singh, I. Fedin, A. S. Fuhr, and V. I. Klimov, *Nat. Energy*, **55**: 409 (2020).
 20. R. Carron, S. Nishiwaki, T. Feurer, R. Hertwig, E. Avancini, J. Löckinger, and A. N. Tiwari, *Adv. Energy Mater.*, **9**, Iss. **24**: 1900408 (2019).
 21. G. Birant, J. de Wild, M. Meuris, J. Poortmans, and B. Vermang, *Appl. Sci.*, **9**: 677 (2019).
 22. Q. Han, Y. T. Hsieh, L. Meng, J. L. Wu, P. Sun, E. P. Yao, and Y. Yang, *Science*, **361**: 904 (2018).
 23. M. Jošt, T. Bertram, D. Koushik, J. A. Marquez, M. A. Verheijen, M. D. Heinemann, and S. Albrecht, *ACS Energy Lett.*, **4**, No. **2**: 583 (2019).
 24. Y. Zhao, S. Yuan, Q. Chang, Z. Zhou, D. Kou, W. Zhou, and S. Wu, *Adv. Funct. Mater.*, **31**, No. **10**: 2007928 (2021).
 25. Y. H. Chang, R. Carron, M. Ochoa, A. N. Tiwari, J. R. Durrant, and L. Steier, *Adv. Funct. Mater.*, **31**, Iss. **40**: 2103663 (2021).
 26. L. Miaomiao, C. Fanggao, L. Chao, X. Cunjun, W. Tianxing, and W. Jihao, *Procedia Eng.*, **27**: 12 (2012).
 27. J. Lindahl, U. Zimmermann, and P. Szaniawski, *IEEE Journal of Photovoltaics*, **3**, Iss. **3**: 1100 (2013).
 28. M. Venkatachalam, M. D. Kannan, S. Jayakumar, R. Balasundaraprabhu, and

- N. Muthukumarasamy, *Thin Solid Films*, **516**, Iss. 20: 6848 (2008).
29. Y. Zhao, H. Li, and Y. Zhu, *Nanoscale Res. Lett.*, **9**: 650 (2014).
 30. Y. Suchikova, A. Lazarenko, S. Kovachov, Z. Karipbaev, and A. I. Popov, *TCSET 2022*, 410 (2022).
 31. M. Sathya, G. Selvan, M. Karunakaran, K. Kasirajan, S. Usha, M. Logitha, and P. Baskaran, *Eur. Phys. J. Plus*, **138**, Article number 67 (2023).
 32. Q. Cui, X. Gu, Y. Zhao, K. Qi, and Y. Yan, *J. Taiwan Inst. Chem. Eng.*, **142**: 104679 (2023).
 33. R. G. Poeira, A. Pérez-Rodríguez, A. J. Prot, M. Alves, P. J. Dale, and S. Sadewasser, *Mater. Des.*, **225** (2023).
 34. R. Fukuda, T. Nishimura, and A. Yamada, *Prog. Photovoltaics*, **31**, Iss. 7: 678 (2023).
 35. X. Jin, R. Schneider, E. Müller, M. Falke, R. Terborg, D. Hariskos, and D. Gerthsen, *Microsc. Microanal.*, **29**, Iss. 1: 69 (2023).
 36. T. Hölscher, M. Placidi, I. Becerril-Romero, R. Fonoll-Rubio, V. Izquierdo-Roca, A. Thomere, and A. Pérez-Rodríguez, *Sol. Energy Mater. Sol. Cells*, **251**: 112169 (2023).
 37. V. Bhatt, S. T. Kim, M. Kumar, H. J. Jeong, J. Kim, J. H. Jang, and J. H. Yun, *Thin Solid Films*, **767**: 139673 (2023).
 38. S. Cheng, K. Zhang, J. Chen, S. Lin, Y. Yao, Y. Sun, and W. Liu, *Appl. Surf. Sci.*, **616**: 156555 (2023).
 39. W. Septina, Y. Kawasaki, T. Harada, and S. Ikeda, *J. Cryst. Growth*, **602**: 126975 (2023).
 40. C. Rincon and F. J. Ramirez, *J. Appl. Phys.*, **72**, Iss. 9: 4321 (1992).
 41. J. P. Van der Ziel, A. E. Meixner, H. M. Kasper, and J. A. Ditzenberger, *Phys. Rev. B*, **9**: 4286 (1974).
 42. S. Roy, P. Guha, S. N. Kundu, H. Hanzawa, S. Chaudhuri, and A. K. Pal, *Mater. Chem. Phys.*, **73**, Iss. 1: 24 (2002).
 43. I. V. Bodnar, A. G. Karoza, and G. F. Smirnova, *Phys. Status Solidi (b)*, **84**, Iss. 1: k65 (1977).
 44. G. D. Holah, A. A. Schenk, S. Perkowitz, and R. D. Tomlinson, *Phys. Rev. B*, **23**, Iss. 12: 6288 (1981).
 45. N. J. Ianno, R. J. Soukup, T. Santero, C. Kamler, J. Huguenin-Love, S. A. Darveau, and C. L. Exstrom, *MRS Online Proceedings Library*, **1012**: 321 (2007).
 46. A. Tverjanovich, S. Bereznev, A. Gertsin, G. Muradova, A. Shoka, D. Kim, and J. Tveryanovich, *Mater. Sci. Appl. Chem.*, **21** (2010).
 47. T. Schmid, N. Schäfer, S. Levchenko, T. Rissom, and D. Abou-Ras, *Sci. Rep.*, **5**: 18410 (2015).
 48. M. Ould Salem, R. Fonoll, S. Giraldo, Y. Sanchez, M. Placidi, V. Izquierdo-Roca, and Z. Jehl Li-Kao, *Solar RRL*, **4**, Iss. 11: 2000284 (2020).
 49. M. Wang, M. Hossain, and K. L. Choy, *Sci. Rep.*, **7**: 6788 (2017).
 50. J. Luo, L. Tang, S. Wang, H. Yan, W. Wang, Z. Chi, and X. Xiao, *Chem. Eng. J.*, **455**: 140960 (2023).
 51. S. Cheng, K. Zhang, J. Chen, S. Lin, Y. Yao, Y. Sun, and W. Liu, *Appl. Surf. Sci.*, **616**: 156555 (2023).